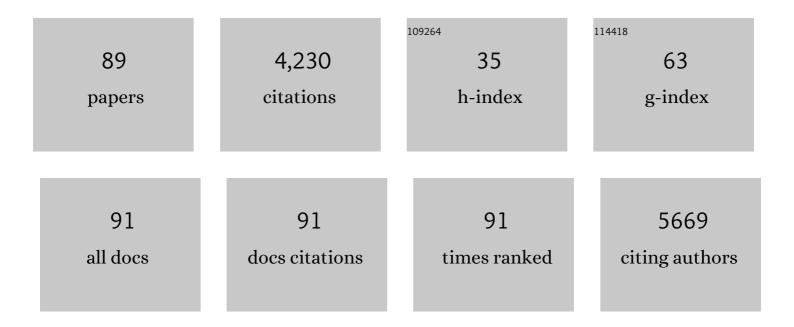
List of Publications by Year in descending order

Source: https://exaly.com/author-pdf/697817/publications.pdf Version: 2024-02-01



LUNFENC LU

#	Article	IF	CITATIONS
1	Self-powered high-performance flexible GaN/ZnO heterostructure UV photodetectors with piezo-phototronic effect enhanced photoresponse. Nano Energy, 2022, 94, 106945.	8.2	73
2	Realizing single-mode lasing in all-inorganic CsPbBr3 perovskite microwires using intrinsic self-absorption. Applied Physics Letters, 2022, 120, .	1.5	2
3	Single-mode lasing of CsPbBr <sub>3</sub> perovskite NWs enabled by the Vernier effect. Nanoscale, 2021, 13, 4432-4438.	2.8	25
4	Wavelength tunable single-mode lasing from cesium lead halide perovskite microwires. Applied Physics Letters, 2021, 118, .	1.5	11
5	Thermal effect induced dynamically lasing mode tuning in GaN whispering gallery microcavities. Journal Physics D: Applied Physics, 2021, 54, 255103.	1.3	4
6	Dynamic regulating of lasing mode in a whispering-gallery microresonator by thermo-optic effect. Applied Physics Letters, 2021, 119, .	1.5	4
7	10.1063/5.0062761.1., 2021, , .		0
8	Photoelectric dual-mode strain sensing based on piezoelectric effect. Journal of Luminescence, 2021, 238, 118237.	1.5	4
9	A ZnO micro/nanowire-based photonic synapse with piezo-phototronic modulation. Nano Energy, 2021, 89, 106282.	8.2	26
10	Reversible Conversion between Schottky and Ohmic Contacts for Highly Sensitive, Multifunctional Biosensors. Advanced Functional Materials, 2020, 30, 1907999.	7.8	61
11	Triboelectric Nanogenerator Enhanced Schottky Nanowire Sensor for Highly Sensitive Ethanol Detection. Nano Letters, 2020, 20, 4968-4974.	4.5	58
12	Strain-modulated high-quality ZnO cavity modes on different crystal orientations. Nanotechnology, 2020, 31, 225202.	1.3	0
13	Piezoelectricity in Multilayer Black Phosphorus for Piezotronics and Nanogenerators. Advanced Materials, 2020, 32, e1905795.	11.1	84
14	Dynamically Modulated GaN Whispering Gallery Lasing Mode for Strain Sensor. Advanced Functional Materials, 2019, 29, 1905051.	7.8	56
15	Brightness improvement in a graphene inserted GaN/ZnO heterojunction light emitting diode. Journal Physics D: Applied Physics, 2019, 52, 395104.	1.3	4
16	Ultrabroadband, Large Sensitivity Position Sensitivity Detector Based on a Bi <sub>2</sub> Te <sub>2.7</sub> Se <sub>0.3</sub> /Si Heterojunction and Its Performance Improvement by Pyroâ€Phototronic Effect. Advanced Electronic Materials, 2019, 5, 1900786.	2.6	33
17	Two Photon–Pumped Whisperingâ€Gallery Mode Lasing and Dynamic Regulation. Advanced Science, 2019, 6, 1900916.	5.6	9
18	Achieving high-resolution pressure mapping via flexible GaN/ ZnO nanowire LEDs array by piezo-phototronic effect. Nano Energy, 2019, 58, 633-640.	8.2	120

#	Article	lF	CITATIONS
19	Crystal-Orientation-Related Dynamic Tuning of the Lasing Spectra of CdS Nanobelts by Piezoelectric Polarization. ACS Nano, 2019, 13, 5049-5057.	7.3	21
20	Controllable Growth of Aligned Monocrystalline CsPbBr <sub>3</sub> Microwire Arrays for Piezoelectricâ€Induced Dynamic Modulation of Singleâ€Mode Lasing. Advanced Materials, 2019, 31, e1900647.	11.1	76
21	Controlled fabrication, lasing behavior and excitonic recombination dynamics in single crystal CH3NH3PbBr3 perovskite cuboids. Science Bulletin, 2019, 64, 698-704.	4.3	33
22	Dynamic regulating of single-mode lasing in ZnO microcavity by piezoelectric effect. Materials Today, 2019, 24, 33-40.	8.3	32
23	Plasmon-enhanced ZnO whispering-gallery mode lasing. Nano Research, 2018, 11, 3050-3064.	5.8	61
24	Optical performance improvement in hydrothermal ZnO/graphene structures for ultraviolet lasing. Journal of Materials Chemistry C, 2018, 6, 3240-3244.	2.7	13
25	Self-assembled ZnO/Ag hollow spheres for effective photocatalysis and bacteriostasis. Materials Research Bulletin, 2018, 98, 64-69.	2.7	71
26	Extra green light induced ZnO ultraviolet lasing enhancement assisted by Au surface plasmons. Nanoscale, 2018, 10, 623-627.	2.8	41
27	Template-free synthesis of porous ZnO/Ag microspheres as recyclable and ultra-sensitive SERS substrates. Applied Surface Science, 2018, 427, 830-836.	3.1	74
28	Piezoelectric Effect Tuning on ZnO Microwire Whispering-Gallery Mode Lasing. ACS Nano, 2018, 12, 11899-11906.	7.3	51
29	Large and Ultrastable Allâ€Inorganic CsPbBr <sub>3</sub> Monocrystalline Films: Lowâ€Temperature Growth and Application for Highâ€Performance Photodetectors. Advanced Materials, 2018, 30, e1802110.	11.1	94
30	In <sub>2</sub> O <sub>3</sub> Nanowire Field-Effect Transistors with Sub-60 mV/dec Subthreshold Swing Stemming from Negative Capacitance and Their Logic Applications. ACS Nano, 2018, 12, 9608-9616.	7.3	32
31	Progress in piezotronic and piezo-phototronic effect of 2D materials. 2D Materials, 2018, 5, 042003.	2.0	62
32	Tunable single-mode lasing in a single semiconductor microrod. Optics Express, 2018, 26, 30021.	1.7	6
33	Synergistic graphene/aluminum surface plasmon coupling for zinc oxide lasing improvement. Nano Research, 2017, 10, 1996-2004.	5.8	23
34	Underlying mechanism of blue emission enhancement in Au decorated p-GaN film. RSC Advances, 2017, 7, 15071-15076.	1.7	10
35	Crystal structure and electron transition underlying photoluminescence of methylammonium lead bromide perovskites. Journal of Materials Chemistry C, 2017, 5, 7739-7745.	2.7	58
36	Plasmon-Induced Accelerated Exciton Recombination Dynamics in ZnO/Ag Hybrid Nanolasers. ACS Photonics, 2017, 4, 2419-2424.	3.2	38

#	Article	IF	CITATIONS
37	Optical Field Confinement Enhanced Single ZnO Microrod UV Photodetector. Chinese Physics Letters, 2017, 34, 078503.	1.3	3
38	Highâ€Altitude Aeolian Research on the Tibetan Plateau. Reviews of Geophysics, 2017, 55, 864-901.	9.0	87
39	Interconnected SnO2 Microsphere Films with Improved Ultraviolet Photodetector Properties. Journal of Electronic Materials, 2017, 46, 6669-6676.	1.0	8
40	Plasmon enhancement for Vernier coupled single-mode lasing from ZnO/Pt hybrid microcavities. Nano Research, 2017, 10, 3447-3456.	5.8	25
41	Magnitude of Species Diversity Effect on Aboveground Plant Biomass Increases Through Successional Time of Abandoned Farmlands on the Eastern Tibetan Plateau of China. Land Degradation and Development, 2017, 28, 370-378.	1.8	15
42	Lasing mode regulation and single-mode realization in ZnO whispering gallery microcavities by the Vernier effect. Nanoscale, 2016, 8, 16631-16639.	2.8	54
43	Tripleâ€Mode Emission of Carbon Dots: Applications for Advanced Antiâ€Counterfeiting. Angewandte Chemie - International Edition, 2016, 55, 7231-7235.	7.2	625
44	Tripleâ€Mode Emission of Carbon Dots: Applications for Advanced Anti ounterfeiting. Angewandte Chemie, 2016, 128, 7347-7351.	1.6	467
45	Plasmon-enhanced Electrically Light-emitting from ZnO Nanorod Arrays/p-GaN Heterostructure Devices. Scientific Reports, 2016, 6, 25645.	1.6	42
46	Tailored Fabrication of <i>α</i> -Fe <sub>2</sub> O <sub>3</sub> Nanocrystals/Reduced Graphene Oxide Nanocomposites with Excellent Electromagnetic Absorption Property. Journal of Nanoscience and Nanotechnology, 2016, 16, 12590-12601.	0.9	14
47	Burstein-Moss Effect Behind Au Surface Plasmon Enhanced Intrinsic Emission of ZnO Microdisks. Scientific Reports, 2016, 6, 36194.	1.6	48
48	SERS-active ZnO/Ag hybrid WGM microcavity for ultrasensitive dopamine detection. Applied Physics Letters, 2016, 109, .	1.5	40
49	Functional group dominance and not productivity drives species richness. Plant Ecology and Diversity, 2016, 9, 141-150.	1.0	16
50	Comparative investigation on temperature-dependent photoluminescence of CH <sub>3</sub> NH <sub>3</sub> PbBr <sub>3</sub> and CH(NH <sub>2</sub> ) <sub>2</sub> PbBr <sub>3</sub> microstructures. Journal of Materials Chemistry C, 2016, 4, 4408-4413.	2.7	109
51	Influence of the gap ratio on variations in the surface shear stress and on sand accumulation in the lee of two side-by-side obstacles. Environmental Earth Sciences, 2016, 75, 1.	1.3	11
52	Dual-band Fabry-Perot lasing from single ZnO microbelt. Optical Materials, 2016, 60, 366-372.	1.7	11
53	Plasmon-mediated exciton–phonon coupling in a ZnO microtower cavity. Journal of Materials Chemistry C, 2016, 4, 7718-7723.	2.7	13
54	Rücktitelbild: Tripleâ€Mode Emission of Carbon Dots: Applications for Advanced Antiâ€Counterfeiting (Angew. Chem. 25/2016). Angewandte Chemie, 2016, 128, 7384-7384.	1.6	9

#	Article	IF	CITATIONS
55	Pattern analysis of a linear dune field on the northern margin of Qarhan Salt Lake, northwestern China. Journal of Arid Land, 2016, 8, 670-680.	0.9	14
56	3D Ag/ZnO hybrids for sensitive surface-enhanced Raman scattering detection. Applied Surface Science, 2016, 365, 291-295.	3.1	46
57	Green emission and Ag <sup>+</sup> sensing of hydroxy double salt supported gold nanoclusters. Nanoscale, 2016, 8, 5120-5125.	2.8	14
58	Energy band modification for UV photoresponse improvement in a ZnO microrod-quantum dot structure. RSC Advances, 2016, 6, 687-691.	1.7	7
59	Facile synthesis of highly conductive sulfur-doped reduced graphene oxide sheets. Physical Chemistry Chemical Physics, 2016, 18, 1125-1130.	1.3	103
60	The excitonic photoluminescence mechanism and lasing action in band-gap-tunable CdS <sub>1â^'x</sub> Se <sub>x</sub> nanostructures. Nanoscale, 2016, 8, 804-811.	2.8	22
61	Nanoplate-Built ZnO Hollow Microspheres Decorated with Gold Nanoparticles and Their Enhanced Photocatalytic and Gas-Sensing Properties. ACS Applied Materials & Interfaces, 2015, 7, 11824-11832.	4.0	89
62	Improved UV photoresponse of ZnO nanorod arrays by resonant coupling with surface plasmons of Al nanoparticles. Nanoscale, 2015, 7, 3396-3403.	2.8	157
63	Optical and Exciton Dynamical Properties of a Screw-Dislocation-Driven ZnO:Sn Microstructure. ACS Applied Materials & Interfaces, 2015, 7, 12655-12662.	4.0	8
64	Single Mode ZnO Whispering-Gallery Submicron Cavity and Graphene Improved Lasing Performance. ACS Nano, 2015, 9, 6794-6800.	7.3	78
65	Grain-size characteristics of linear dunes on the northern margin of Qarhan Salt Lake, northwestern China. Journal of Arid Land, 2015, 7, 438-449.	0.9	16
66	Plasmon coupled Fabry-Perot lasing enhancement in graphene/ZnO hybrid microcavity. Scientific Reports, 2015, 5, 9263.	1.6	36
67	Spatial variability of vegetation characteristics, soil properties and their relationships in and around China's Badain Jaran Desert. Environmental Earth Sciences, 2015, 74, 6847-6858.	1.3	21
68	Plasmon-Enhanced Whispering Gallery Mode Lasing from Hexagonal Al/ZnO Microcavity. ACS Photonics, 2015, 2, 73-77.	3.2	54
69	Lasing behavior modulation in a layered cylindrical microcavity. Applied Physics B: Lasers and Optics, 2015, 118, 93-100.	1.1	3
70	Improved Whispering-Gallery Mode Lasing of ZnO Microtubes Assisted by the Localized Surface Plasmon Resonance of Au Nanoparticles. Science of Advanced Materials, 2015, 7, 1156-1162.	0.1	22
71	Tunable blue and orange emissions of ZnS:Mn thin films deposited on GaN substrates by pulsed laser deposition. Journal of Luminescence, 2014, 147, 310-315.	1.5	21
72	The effect of desertification on carbon and nitrogen status in the northeastern margin of the Qinghai-Tibetan Plateau. Environmental Earth Sciences, 2014, 71, 807-815.	1.3	19

JUNFENG LU

#	Article	IF	CITATIONS
73	Direct Resonant Coupling of Al Surface Plasmon for Ultraviolet Photoluminescence Enhancement of ZnO Microrods. ACS Applied Materials & Interfaces, 2014, 6, 18301-18305.	4.0	69
74	Aeolian transport over a developing transverse dune. Journal of Arid Land, 2014, 6, 243-254.	0.9	14
75	Driving forces of aeolian desertification in the source region of the Yellow River: 1975–2005. Environmental Earth Sciences, 2013, 70, 3245-3254.	1.3	28
76	Geomorphology of star dunes in the southern Kumtagh Desert, China: control factors and formation. Environmental Earth Sciences, 2013, 69, 267-277.	1.3	15
77	Effects of Au catalysts for synthesis of ZnS microstructures on the sapphire substrate. Materials Letters, 2013, 93, 337-340.	1.3	5
78	Size Effects of Raman and Photoluminescence Spectra of CdS Nanobelts. Journal of Physical Chemistry C, 2013, 117, 20998-21005.	1.5	105
79	Phase controlled synthesis and optical properties of ZnS thin films by pulsed laser deposition. Materials Research Bulletin, 2013, 48, 3843-3846.	2.7	29
80	Synthesis and investigation of blue and green emissions of ZnS ceramics. Journal of Luminescence, 2013, 134, 498-503.	1.5	37
81	Preparation and Photoluminescence of (3C-ZnS)/(2H-ZnS) Superlattice in Mn-doped ZnS Nanoribbons. Journal of Physical Chemistry C, 2012, 116, 23013-23018.	1.5	19
82	Controlled growth and photoluminescence of one-dimensional and platelike ZnS nanostructures. Applied Surface Science, 2012, 258, 8538-8541.	3.1	17
83	Driving forces responsible for aeolian desertification in the source region of the Yangtze River from 1975 to 2005. Environmental Earth Sciences, 2012, 66, 257-263.	1.3	30
84	Mean airflow patterns upwind of topographic obstacles and their implications for the formation of echo dunes: A wind tunnel simulation of the effects of windward slope. Journal of Geophysical Research, 2011, 116, .	3.3	19
85	The significance of Gobi desert surfaces for dust emissions in China: an experimental study. Environmental Earth Sciences, 2011, 64, 1039-1050.	1.3	23
86	Equations for the nearâ€surface mass flux density profile of windâ€blown sediments. Earth Surface Processes and Landforms, 2011, 36, 1292-1299.	1.2	29
87	Monitoring land use and land cover change in the source region of the Yangtze River using multi-temporal Landsat data. , 2011, , .		1
88	Aeolian desertification and its causes in the Zoige Plateau of China's Qinghai–Tibetan Plateau. Environmental Earth Sciences, 2010, 59, 1731-1740.	1.3	88
89	Graphene induced lasing mode tailoring in GaN floating microring cavity. Europhysics Letters, 0, , .	0.7	Ο